Identification and characterization of an inhibitory Fibroblast growth factor receptor 2 (FGFR2) molecule, upregulated in an Apert Syndrome mouse model

Lee M Wheldon, Naila Khodabukus, Susannah J Patey, Terence G Smith, Jk Heath, Mohammad K Hajihosseini

Biochemical Journal Immediate Publication. Published on 28 Feb 2011 as manuscript BJ20100884

Identification and characterization of an inhibitory Fibroblast growth factor receptor 2 (FGFR2) molecule, upregulated in an Apert Syndrome mouse model

Lee M. Wheldon[1¶], Naila Khodabukus[1], Susannah J. Patey[1], Terence G. Smith,[2] John K. Heath[1] and Mohammad K. Hajihosseini[2§]

[1]School of Biosciences, University of Birmingham, Edgbaston, B15 2TT, UK.
[2]School of Biological Sciences, University of East Anglia, Norwich, Norfolk, NR4 7TJ, UK.

[¶] Present address: MBIG, Centre for Biomolecular Sciences, University of Nottingham, Nottingham, NG7 2RD, UK.

[§] Corresponding author: M. K. Hajihosseini, School of Biological Sciences, University of East Anglia, Norwich, Norfolk, NR4 7TJ, UK.
Tel: +44 – 01603 – 591318
Fax: +44 – 01603 –592250
Email: m.k.h@uea.ac.uk

Running title: an inhibitory FGFR2 molecule

Keywords: Fibroblast growth factor receptors; mRNA splicing; Apert syndrome, Mouse.

Biochemical Journal Immediate Publication. Published on 28 Feb 2011 as manuscript BJ20100884

ABSTRACT

Apert syndrome (AS) is a congenital disease composed of skeletal, visceral and neural abnormalities, caused by dominant-acting mutations in FGFR2. Multiple FGFR2 splice variants are generated through alternative splicing, including premature termination codon (PTC)-containing transcripts that are normally eliminated via the nonsense mediated decay (NMD) pathway. We have discovered that a soluble truncated FGFR2 molecule encoded by a PTC-containing transcript is upregulated and persists in tissues of an Apert syndrome mouse model. We have termed this IIIa-TM as it arises from aberrant splicing of FGFR2 exon 7 (IIIa) into exon 10 (transmembrane domain). IIIa-TM is glycosylated and can modulate the binding of FGF1 to FGFR2 molecules in BIAcore binding assays. We also show that IIIa-TM can negatively regulate FGF signalling in vitro and in vivo. Apert syndrome phenotypes are thought to result from gain-of-FGFR2 signalling, but our findings suggest that IIIa-TM can contribute to these through a loss-of-FGFR2 function mechanism. Moreover, our findings raise the interesting possibility that FGFR2 signalling may be a regulator of NMD pathway.

INTRODUCTION

Loss-of-function studies have demonstrated that Fibroblast growth factor (FGF) signalling is a critical mediator of cellular interactions that underlie tissue development, repair and homeostasis. For example, the growth of lungs and limbs is arrested in Fgf10-null embryos and adult FGF23-deficient mice develop hyperphosphataemia [1, 2]. However, subtle defects can also arise from partial-loss or gain-of-FGF signalling, suggesting that the level of FGF signal perceived by target cells is also important [3-5]. This is exemplified by Apert and Pfeiffer syndromes, which are hallmarked by a host of skeletal, visceral and neural defects arising from dominant-acting mutations in FGF Receptors (FGFRs) -1 and -2 [6]. Therefore, identifying the set of factors and mechanisms that regulate the dynamics of FGF signalling will further our understanding of growth factor signalling in developmental and disease processes.

The mammalian FGF signalling system is comprised of 18 FGF ligands and four transmembrane FGFRs (1-4), and can operate both in a morphogen and a threshold-dependent signalling manner [7-9]. Formation of a trimeric complex of FGFs, sulphated proteoglycans and membrane-anchored FGFR molecules results in the recruitment of intracellular adaptor proteins by the activated FGFRs, and signal transduction to the nucleus via the MAP kinase (MAPK), PI-3 kinase or phospholipase C signalling pathways. Typically, FGF signalling induces changes in gene expression and/or cytoskeletal reorganization to regulate multiple aspects of cell behaviour and fate. The level and threshold of FGF signalling is modulated intracellularly through the activity of proteins such as Sprouty, MKP3, Spred and Sef, and by the synergistic or antagonistic effects of other signalling pathways – Notch, Wnts, BMPs, Hedgehogs etc. [5, 10]. Extracellular regulation, by contrast, is dependent mostly on the bioavailability of FGFs and FGFRs, as well as factors that modulate their interactions such as FLRTs and Klotho [11, 12].

FGFR molecules are typically composed of two or three extracellular immunoglobulin-like domains (Ig-I, Ig-II and Ig-III) harbouring the ligand-binding sites; a single pass transmembrane domain (TM); an intracellular juxta-membrane domain; and a split tyrosine kinase domain. Alternative splicing of FGFR transcripts generates multiple receptor isoforms and contributes to the functional diversity of FGF signalling [7, 13]. For example, the VT+ or VT- isoforms of FGFR1, which harbor or lack amino-acids V428 and T429 in the juxta-membrane domain, engage different signalling pathways [14]. Moreover, the so-called 'IIIb' and 'IIIc' spliced isoforms of FGFRs 1-3 are formed through alternative usage of exons 8 and 9, which encode the C-terminal half of Ig-III [15] ie. exon 7(IIIa)-8(IIIb)-10(TM) or exon 7(IIIa)-9(IIIc)-10(TM) splice variants. These isoforms play critical roles in the paracrine cross talk between epithelial and mesenchymal cells, since IIIb isoforms are predominant in the former and activated by mesenchymally-produced FGF ligands (FGFs 3, 7, 10 and 22), whilst the IIIc receptor isoforms are expressed by mesenchymal (and neural cells) and activated by a different set of FGFs (FGFs -2, -4, -8, -9 and 18), produced by epithelial cells [16].

Less clear is the biological significance of soluble FGFR isoforms. These include a molecule that specifically lacks the TM domain, or truncated receptors that harbour Ig-II and Ig-IIIa, with or without fusion to the first 3 amino acids of the TM domain or non-coding intronic sequences [7, 17, 18]. Some of these truncated receptors are encoded by PTC-containing transcripts [7], and are likely eliminated by the nonsense-mediated decay pathway machinery (NMD; [19]).

Through gene targeting in ES cells, we had previously generated mice with an Apert syndrome-type FGFR2 mutation [20]. In these, as in some patients, a heterozygous deletion of FGFR2-exon 9 (IIIc) (ie. FgfR2-IIIc$^{+/\Delta}$), results in the aberrant co-expression of FgfR2-IIIb and FgfR2-IIIc isoforms in mesenchymal and neural cells [21, 22]. Consequently, the affected tissues become promiscuously responsive to a broader set of FGF ligands and a gain-of-FGFR2 function ensues. We validated this mechanism by showing that much of the Apert-like phenotypes in FgfR2-IIIc$^{+/\Delta}$ mice can be rescued merely by knocking down the levels of Fgf10, a key FgfR2-IIIb activating ligand [23].

We now report that FgfR2-IIIc$^{+/\Delta}$ tissues additionally harbour a PTC-derived truncated FgfR2 molecule that we term 'IIIa-TM'. IIIa-TM arises from direct splicing of exon 7(IIIa) into 10(TM) to encode a molecule that harbours the Ig-I, Ig-II and the amino-half of Ig-III (IIIa) domains fused to the first 3 amino-acids of TM. We have explored the biochemical properties of IIIa-TM and find that it has some ligand binding capacity. Moreover, IIIa-TM is capable of attenuating basal FGFR signalling in vitro and in vivo, and influences the trafficking of endogenous FGFR2 molecules. Our findings suggest that IIIa-TM escapes NMD and acts as a negative regulator of FGFR signalling to cause or contribute to the severity of phenotypes in Apert syndrome, which were otherwise thought to arise solely through gain-of-FGFR2 activity.

METHODS

Animals and tissue source, FgfR2-IIIc$^{floxed/+}$ and PGK-cre mice were used to derive the FgfR2-IIIc$^{+/\Delta}$ mutant mice/ tissues, as previously described [20, 23]. All mice were bred and maintained on C57BL background in accordance with Home Office licences and local regulations governing animal welfare and ethics.

Detection, isolation and cloning of IIIa-TM – RNA was isolated from brains of newborn wild type or FgfR2-IIIc$^{+/\Delta}$ (mutant) mice using Tri reagent (Sigma), and subjected to two-step RT-PCR reaction using Ready-to-Go beads (Amersham-Pharmacia) and previously-described cycle conditions [20, 24]. IIIa-TM transcript (Fig. 1A) was detected using Primers P1 (5'-CCCATCCTCCAAGCTGGACTGCCT-3') and P2 (5'-GCTTGGTCAGCTTGTGCACAGCTGG-3'). 'Full length' FGFR2-IIIa-TM was amplified using *NdeI*-tagged primer P3 (5'-AGTTTAGTTGAGGATACCACTTTAG-3') in conjunction with *NotI*-tagged primer P4 (5'-TCACAGGCGCTTCAGGACCTTG-3'). Products were sequenced using forward or reverse complements of primers P1 and P5 (5'-CGTGATCAGTTGGACTAAGGATGG-3'; nucleotides 815-835 of FgfR2, NM_010207) (Supplementary Fig. 1). A 0.9Kb recombinant IIIa-TM was generated by primers P2 and P3, gel purified, and cloned into a 7.9 Kb ires-Topaz-pEF-BOS plasmid, downstream of sequences encoding human FGFR2 secretory signal sequence, IgG-FC, and a 3C-protease-sensitive site, respectively (Supplementary Fig. 2). To examine the distribution of native IIIa-TM protein, lungs or brains of wild type and mutant newborn mice were triturated through a 19G gauge needle and protein was extracted by 30 mins incubation at 4°C in 500μl RIPA buffer containing protease inhibitor cocktail (Roche). Tissue lysates were cleared by centrifugation (20,800*g*, 60 min, 4°C) and protein concentrations determined by Coomassie assay (Pierce).

Maintenance and transfection of cell lines - Human embryonic kidney 293T and Cos7 cells were maintained at 37°C in a humidified atmosphere of 5% CO_2, in

Dulbecco's Modified Eagle's Media, supplemented with 10% foetal calf serum, 2mM L-glutamine, 1mM sodium pyruvate, 0.2 U/ml penicillin and 0.1mg/ml streptomycin. 70% confluent plates of 293T cells were transiently transfected by the calcium phosphate precipitation method overnight with plasmid DNA (30, 60 or 300μg) diluted in 2M $CaCl_2$ and 2x HBS (1.6% NaCl; 1.2% Hepes; 0.04% Na_2HPO_4; pH 7.12). Cells were then washed with serum-free media and maintained in the same or Ultracho media (Biowhittaker).

Antibodies used - Primary: sheep anti-FGFR2 N-terminal (Nt; 1:2000 – 10000; Anderson and Heath, unpublished [24]); Rabbit anti-FGFR2 cytoplasmic (Bek C-17, 1:500-1000, Santa Cruz); Mouse anti-ERK and anti-phospho-ERK (1:1000 and 1:2000, respectively; Cell Signalling Inc); mouse anti-Lamp2 (1:50, Abcam); and Horseradish Peroxidase (HRP) conjugated goat anti-human Fc (1:10000, Pierce). Secondary: HRP-conjugated anti-mouse, -rabbit (1:5000, Amersham Biosciences) and -sheep antibodies (1:4000, The Binding Site); FITC-conjugated anti-rabbit (1:300), and Texas Red-conjugated anti-mouse (1:200) antibodies (Molecular Probes).

Immunodetection and quantitation of FGFR2 and Lamp2 co-localization. Cos7 cells were grown on glass coverslips and transfected with FGFR2 using Genejuice (Invitrogen). 48 hours later, cells were fixed with 4% paraformaldehyde (10 min), permeabilised with cold methanol and re-hydrated in PBS. After 1hr incubation in PBS/4% BSA, the cells were exposed to anti-Lamp2 and anti-Bek antibodies for 1hr. Coverslips were then washed in PBS and incubated with the relevant secondary antibodies for 1 hour, washed in PBS/0.1%/Tween-20 and mounted using Mowiol medium. Images of immunolabelled cells were captured using a confocal microscope (Leica), processed in Adobe photoshop and merged using ImageJ. To quantitate co-localization of FGFR2 and Lamp2, 15 random images from different treatments across 2 different experiments were analysed and a co-efficient was determined using ZEN 2009 software. Mean values (± SEM) were subjected to Student t-test. One way ANOVA indicated no variance with respect to time of FGF2 stimulation in the absence of IIIa-TM (see Fig. 5A for paradigm) but a significant difference in its presence (*p,0.05;***p,0.0001). Dunnett's Multiple comparison Test also confirmed a significant abrogation of FGFR2/Lamp2 co-localization in the presence of IIIa-TM only.

Immunoprecipitation of FGFR2 - Protein was extracted from pellets of transiently-transfected 293T cells by a 30 min incubation in a lysis buffer containing protease inhibitor cocktail (Roche)). After removing cell debris, the Triton-insoluble fraction was isolated by centrifugation and FGFR2 was immunoprecipitated from the supernatant with 3.5μg of anti-FGFR2 (Bek) antibodies for 1 hour at 4ºC. Immuno-complexes were captured with 50% protein-A-sepharose slurry for 30 min at 4ºC and samples were washed twice with ice-cold hcTBST (100mM Tris base, 1.5M NaCl, 0.05% Tween-20, pH 7.4) followed by ice-cold TE buffer. The resultant samples were boiled for 5 mins and subjected to SDS-PAGE and immunoblotting analyses.

SDS-PAGE and protein detection - Proteins were loaded onto SDS-PAGE and transferred to nitrocellulose membranes (Protran BA85 – Schleicher & Schuell) using a Biometra semi-dry transfer system, at 5mA/cm^2 of gel for 25 min. Membranes were blocked overnight at 4°C with TBS-T/5% BSA (TBST; 20mM Tris base; 140mM NaCl; 0.1% Tween-20) and then incubated for 1 hour at RT with the relevant primary antibodies. Secondary antibodies were applied for one 1 at RT and following washes in TBS-T, immunoreactive bands were detected with ECL reagents (Pierce). Where necessary, membranes were stripped in 0.1M Glycine (pH 2.5), washed sequentially

in TBS-T and TBS-T/5% BSA and re-probed overnight at 4°C.

Purification of Fc-tagged proteins - 3CFc, IIIa-TM-3CFc, FGFR2-IIIb-3CFc and FGFR2-IIIc-3CFc proteins were harvested from 293T cells or their conditioned medium, 24 hours (48 hrs for IIIa-TM) after transfection with the relevant plasmids [25]. 3CFc-tagged proteins were purified by gravity flow over a protein A-sepharose fast flow column previously equilibrated with MT-phosphate buffered saline (MT-PBS; 150mM NaCl; 16mM Na_2HPO_4; 4mM NaH_2PO_4). Columns were then washed successively with MT-PBS/1% triton X-100), MT-PBS alone and finally, 50mM Tris-HCl pH 8; 150mM NaCl solution. Proteins were eluted from the column with 0.1M glycine pH 3 and dialysed overnight at 4°C. To obtain cleaved recombinant IIIa-TM, the column was washed with TNED (50mM Tris-HCl pH 8; 150mM NaCl; 10mM EDTA pH 8; 1mM DTT) and treated overnight at 4 C with 10 μg of 3C protease. Cleaved IIIa-TM was then dialysed into PBS.

PNGase-F treatment **-** Purified IIIa-TM protein (1mg) was boiled for 10 min in a solution containing 50mM Tris-HCl pH 8, 150mM NaCl, 10mM EDTA, 1mM DTT, 0.5% SDS and 1% β-mercaptoethanol, and treated for 16 hours at 37ºC with 5U PNGase-F (New England Biolabs) in a solution of 50mM Na_2HPO_4 (pH 7.5) and 1% NP40 (v/v).

2-Dimensional Gel Electrophoresis – 100mg of tissue-extracted protein or 900ng of recombinant IIIa-TM protein, were mixed with 125μl of rehydration buffer (8M Urea; 2% CHAPS; 20mM DTT; 0.5% IPG buffer; trace of bromophenol blue) and loaded into a strip holder. An IPG drystrip (7cm, pH 4-7 immobilised linear gradient – Amersham Pharmacia) was overlaid onto the rehydration buffer containing sample and rehydrated overnight at 20°C**.** Optimal IEF was carried out using an IPGphor, step-n-hold, and the following protocol: 500V for 500Vh, 1000V for 1000Vh and 8000V for 16000Vh, all at 20°C. Strips were then immediately processed for SDS-PAGE or stored at –70°C until required.

For SDS-PAGE, IEF strips were equilibrated for 20 min at a time with Equilibration buffer 1 (50mM Tris-HCL, pH 8.8; 6M urea; 30% glycerol (v/v); 2% SDS (w/v); 60mM DTT and a trace of bromophenol blue) followed by Equilibration buffer 2 (same as buffer 1, but DTT replaced with 25mg/ml iodoacetamide). Drystrips were sealed into wells (0.5% agarose in running buffer) and samples then resolved on vertical SDS-PAGE gels at 110V for 10 min followed by 200V for 30 min. Protein spots were visualised by chemiluminescence after transfer to nitrocellulose as detailed above.

Surface plasmon resonance analysis – All protein interactions were measured using a BIAcore 2000 (Uppsala, Sweden). 3CFc-tagged proteins were immobilized in 10mM sodium acetate pH 4.5 onto a research grade C1 sensor chip (BIAcore) as per manufacturer's instructions) at a flow rate of 10μl/minute. Proteins were immobilized to similar levels (~1000 response units (RUs) above the pre-injection baseline; ~400RU for 3CFc due to M_w difference); the excess carboxyl groups were then blocked by an injection of 70μl 1M ethanolamine, pH 8.5. Binding experiments were performed in HBS-EP (0.01M Hepes pH 7.4, 0.15M NaCl, 3mM EDTA, 0.005% surfactant P-20) (BIAcore) at a flow rate of 50μl /min using varying concentrations of FGF1 ligand (JKH laboratory) and IIIa-TM proteins diluted in HBS-EP. Residual bound FGF and IIIa-TM was removed with injections of 2M NaCl and 10mM HCl. Reference responses from 3CFc flow cells were subtracted for each analyte concentration using BiaEvaluation software (BIAcore AB). Disturbances at the start and end of sensorgrams were excluded from curve fitting analysis. Kinetic and R_{eq} data was derived using four different analyte concentrations and a Langmuir model of binding (1:1) for curve fitting. Following curve fitting, each sensorgram was manually

examined for the closeness of the fit. χ^2 was <10% of R_{max} in all cases.

Chick embryo manipulations and in situ hybridization - The somites of Hamburger and Hamilton (HH) stage 17-21 chick embryos were electroporated with 2mg/ml of purified plasmids encoding IIIa-TM or GFP (as control) using a previously-described protocol [26]. After 5-7 hours of incubation at 37°C, electroporated embryos were fixed in 4% PFA and processed for in situ hybridization using Digoxygenin (Dig) or fluorescene (FL)-tagged anti-sense *Mkp3* or *GFP* riboprobes. In situ signal was detected using alkaline phosphatase tagged anti-Dig and anti-FL antibodies [26]. *GFP* was visualised in orange by using an INT/BCIP solution, while *Mkp3* was visualized in purple with NBT/BCIP solutions (Roche; Fig. 5C). Use of control sense labels did not yield any signal.

RESULTS

Widespread expression and persistence of IIIa-TM in FgfR2-IIIc$^{+/\Delta}$ tissues

Splicing of FgfR2 exon 7(IIIa) into 10(TM) should yield a 317 amino-acid long soluble FGFR2 molecule (IIIa-TM; (Fig 1A)) with a predicted molecular weight of 35.5 kDa (if non-glycosylated) and pI of 5.88. In order to contribute to FgfR2-IIIc$^{+/\Delta}$ (hereon referred to as 'mutants') phenotypes, IIIa-TM should survive NMD and be detectable at both transcript and protein level.

Using standard RT-PCR reactions and primers specific to exons 7(IIIa) and 10(TM), respectively, we detected low levels of IIIa-TM spliced transcripts in RNA derived from the brains of mutant but not wild type mice (Fig. 1B). To examine whether IIIa-TM is present as a 'full length' FGFR2 molecule, we used primers from FGFR2 exon 2 and the IIIa-TM splice junction and successfully amplified an 873 base pair 'full-length' transcript. DNA sequencing confirmed that this product encodes Ig domain I, the 'acid-box', Ig-II, and Ig-IIIa, spliced to the first nine bases of exon 10 (Supplementary Fig 1.). IIIa-TM transcripts were found in diverse tissues and all stages examined, namely, in the mutant embryonic forebrain (E14.5), hindbrain (E9.5), lungs (E14.5) and newborn lung, liver and kidneys – but never in comparable wild type siblings (data not shown).

To examine whether the IIIa-TM transcripts are translated into protein in vivo, we subjected the soluble fraction of protein isolated from wild type and mutant tissues to 2-Dimensional gel analysis over a pI 4-7 range, and probed the resulting blots with antibodies that only detect the ectodomain of FGFR2 (here on termed FGFR2-N-terminal (Nt) antibody). Two major immunoreactive spots of apparent molecular mass of 55 kDa (pI 5.1 and 6.3) and a minor 120 kDa spot (pI 4.3) were detectable in the mutant (Fig. 1C) but not wild type samples. Equal loading of protein in these assays was confirmed by anti-tubulin labelling (data not shown).

Taken together, these findings demonstrate that IIIa-TM is present and could modulate FGF signalling in the mutant tissues.

Biochemical characterization of recombinant IIIa-TM protein

To explore the biochemical and binding properties of IIIa-TM, we generated a recombinant protein. Using RT-PCR, we first amplified a 0.87Kb IIIa-TM cDNA fragment lacking the endogenous FgfR2 signal sequence, and cloned this into an ires-Topaz-pEF-BOS plasmid, downstream of sequences composed of human FGFR2 secretory signal sequence, human IgG-FC, and a 3C-protease-sensitive site, respectively (Fig. 2A; Supplementary Fig. 2). The resulting recombinant protein (hereon termed IIIa-TM-3CFc) was isolated from the supernatant of transiently-transfected 293T cells, using protein-A-sepharose (Fig. 2B). The recombinant IIIa-TM protein was produced optimally at 60 hours post-transfection, but thereafter it was down-regulated or degraded (data not shown).

To further characterise soluble IIIa-TM, the Fc domain of the recombinant IIIa-TM-3CFc was cleaved by 3C protease digestion. We found that in solution the 3C-cleaved IIIa-TM protein forms multiple higher molecular weight products (e.g. 110 kDa) (Fig. 2C), which, in the presence of the reducing agent DTT (200mM), were reduced to a multiple immunoreactive species of approximately 55 kDa (Fig. 2C, lane 2). Likely, these higher order products result from dimeric or oligomeric association of the native ~55 kDa protein, via di-sulphide bonding of the unpaired cysteine residue present on the IgIII domain of IIIa-TM (Fig. 2A), as observed in soluble FGFR1 and FGFR3 molecules [17, 27].

IIIa-TM contains eight putative N-glycosylation sites (Fig. 1A; Supplementary data 1), a subset of which must be glycosylated if IIIa-TM, like other FGFRs, is to interact with FGF ligands. To test this, we removed the N-linked oligosaccharide residues from 3C-cleaved IIIa-TM by PNGase-F (Peptide: N-Glycosylase F) treatment and found that the apparent mass of the native protein is reduced from 55 to 35 kDa (Fig. 2C, lane 3). Moreover, resolution of 293T-derived recombinant IIIa-TM on 2D-gels yielded eight distinct products of different molecular weights and pIs (Fig. 2D), suggesting that these are multiple order glycoforms. These findings can explain why IIIa-TM appears as a broad band on a standard SDS-PAGE gel (Fig. 2C, lane 2) and also raise the possibility that the two spots noted in Fig. 1C represent two different glycoforms of IIIa-TM in the mutant brain, in vivo.

IIIa-TM can modulate the binding kinetics of FGF1 to FGFR2 molecules

As a secreted truncated receptor, IIIa-TM could interfere with FGFR2 signalling either by sequestering FGF ligands away from FGFRs, and/ or forming non-functional hetero-dimers with full-length FGFRs themselves. However, both of these processes require an interaction between FGF ligand/s and IIIa-TM. We therefore used the well-characterised BiAcore assay [28] to investigate the dynamics of such interactions, either in the presence or absence of recombinant FGFR2-IIIb or FGFR2-IIIc ectodomain molecules.

First, a series of Fc-tagged proteins were generated in 293T cells by transfection with plasmids encoding IIIa-TM-3CFc, FGFR2-IIIb-3CFc, FGFR2-IIIc-3CFc, or 3CFc as control. Purified proteins were immobilized onto a BIAcore C1 sensor chip in equimolar amounts and then different concentrations of FGF1 were perfused across the sensor chip in the absence of heparin in order to examine receptor-ligand interactions. FGF1 was chosen, because it interacts with all FGFRs/ FGFR isoforms [16]. BIAcore assays measure the rate of association followed by dissociation of free and chip-anchored proteins. To evaluate these parameters, we obtained the plasmon resonance values and normalised them against values obtained by binding of FGF1 to the control protein, 3CFc.

As shown in Fig. 3 and Table 1, FGF1 bound chip-anchored FGFR2-IIIb and FGFR2-IIIc molecules with similar affinity - K_D 5.14 x 10^{-10} and 7.05 x 10^{-10}, respectively, but showed no discernible binding to chip-anchored IIIa-TM (Fig. 3D). The latter observation is likely explained by the absence of the C-terminal half of Ig-III like domain from IIIa-TM [29].

In the presence of excess free IIIa-TM (i.e. 62.5 nM), however, FGF1 interacted with chip-anchored IIIa-TM (K_D 6.8 x 10^{-8}). Free IIIa-TM also caused more total protein interaction with chip-anchored FGFR2-IIIb and FGFR2-IIIc (Fig. 3G-I) but simultaneously reduced the binding affinity of FGF1 to chip-anchored FGFR2-IIIb and -IIIc by 5 and 10 fold, respectively (Table 1). Importantly, we found that in the absence of FGF1, excess free IIIa-TM does not bind to chip-anchored IIIa-TM, FGFR2-IIIb, or FGFR2-IIIc (Fig. 3A-C).

Taken together, these findings demonstrate that as a complex, IIIa-TM is capable of interacting with FGF1 and modulating its interactions with receptor molecules that contain the entire ligand binding domain. By inference, IIIa-TM may attenuate FGF signalling through two mutually non-exclusive mechanisms: sequestering FGF ligands and/or forming non-functional heterodimers with FGFRs.

Exogenous IIIa-TM modulates the levels of FGFR signalling and trafficking of FGFR2

We next examined whether IIIa-TM alters the dynamics of FGFR signalling in

cultured cells. Cos7 cells, which endogenously express the IIIc of FGFRs -1, -2 and -4 (Fig. 4A) and FGFs –4 and –9 (MKH and LMW, unpublished data) were grown to confluency and serum-starved before being co-stimulated with FGF2 (20ng/ml) and heparin (10μg/ml), in the presence or absence of exogenously added 3C-cleaved IIIa-TM (5μg/ml). Immunoblotting of total cell lysates with anti-ERK and phospho-ERK antibodies, showed that the presence of IIIa-TM reduces the level of FGF signalling (Fig. 4B). Immunoprecipitation of FGFR2 with antibodies against the cytoplasmic domain of FGFR2 (Bek C17) followed by immunoblotting with anti-FGFR2(Nt) or anti-phosphotyrosine (pY20/4G10 cocktail) antibodies revealed a clear inhibition of FGFR phosphorylation levels in the presence of IIIa-TM (Fig. 4C).

Interestingly, we noted a decrease in levels of full-length FGFR2 in cells exposed to IIIa-TM and FGF2 combined (Fig. 4C). This could be explained either by rapid destruction of FGFRs, or more likely, the translocation of FGFRs into a cellular compartment that is detergent-insoluble or inaccessible to the immunoprecipitating antibodies. Nonetheless, these changes demonstrate that exogenously added IIIa-TM can modulate FGFR2-mediated signalling levels in cultured cells.

To investigate how IIIa-TM impacts the trafficking of FGFR2 in cells, we transfected 293T or Cos7 cells, which have low levels of endogenous FGFR2, with full length FGFR2-encoding plasmids before treatment with exogenous IIIa-TM in the presence or absence of FGF2 (Fig. 5A). Co-immunolabelling of cells with anti-FGFR2(Nt) and anti-Lamp2 antibodies and quantitation of their co-localization showed that in the absence of IIIa-TM, significant levels of transfected FGFR2 is internalised into $Lamp2^{+}$ late endosomes and lysosomes, even when cells were treated with FGF2. In the presence of IIIa-TM, however, FGFR2 molecules appear to accumulate at the cell membrane - more so when FGF2 is present – and show reduced association with endosomes/lysosomes (Fig. 5B-H). These findings concur with the BIAcore data and suggest that IIIa-TM forms a complex with FGF ligands and receptors, which in living cells, traps the receptors at the cell surface.

IIIa-TM can attenuate FGF signalling in vivo

Next, we tested whether IIIa-TM can also modulate FGFR signalling in vivo, in chick embryos. We took advantage of previous findings that proper generation of chick somites (precursors to axial muscles) relies on FGFR signalling [26], such that electroporation of a dominant-negative (membrane bound) FGFR construct or the application of FGFR inhibitor, SU5406, can disrupt normal somitogenesis. Attenuation of FGF signalling in this system is measured by the loss of Mkp3 expression, which is a cytoplasmic modulator and a target of FGFR signalling itself [10, 26].

Plasmids encoding IIIa-TM (2 μg/ml) or GFP were electroporated into the developing chick somites and in situ hybridization was used to detect *Gfp* or *Mkp3* in the manipulated embryos (n=2 of each treatment). As shown in Fig. 6, introduction of IIIa-TM but not GFP-encoding plasmids resulted in the loss of Mkp3 expression, which is reminiscent of the attenuation of FGFR signaling by SU5402 or dominant-negative FGFRs [26]. These findings demonstrate that IIIa-TM interferes with FGFR signalling in an in vivo setting.

Biochemical Journal Immediate Publication. Published on 28 Feb 2011 as manuscript BJ20100884

DISCUSSION

In this study we show that a soluble FGFR2 molecule is upregulated in FgfR2-IIIc$^{+/\Delta}$ mice, which model Apert syndrome. We termed this molecule IIIa-TM, as it arises from aberrant splicing of FgfR2 exon 7(IIIa) into exon 10(TM). Neither the transcript, nor IIIa-TM protein were detected in wild type tissues/cells. Recombinant IIIa-TM generated in 293Tcells was found to be N-glycosylated and formed oligomeric complexes in solution. Using BIAcore sensor chip assays we found that IIIa-TM protein displays limited FGF ligand binding. Exogenous addition of IIIa-TM in the presence of FGF ligands efficiently attenuated FGFR signalling and interfered with receptor trafficking in cultured cells. Finally, introduction of IIIa-TM into the developing chick embryos attenuated FGFR signalling. Taken together, these findings suggest that IIIa-TM is in a position to induce loss-of-FgfR signalling in FgfR2-IIIc$^{+/\Delta}$ mice, and by inference in Apert syndrome.

FgfR2 is encoded by 19 exons that can generate a spectrum of alternatively spliced transcripts [7]. IIIa-TM is one such candidate but it was not detected in normal cells either by RT-PCR (this study) or RNAse protection assays [30]. This suggests that either splicing of exon 7 into 10 is a rare event, or more likely, that as a PTC-containing transcript, IIIa-TM is normally destroyed by components of the NMD pathway. In general, NMD machinery eliminates transcripts that carry a PTC positioned greater than 50-55 bp upstream of the last coding splice junction of a gene (see reviews [19, 31]).

Interestingly, NMD is thought to play a critical role in regulating the expression levels of alternatively-spliced genes, whereby the amount of useful transcripts destined for translation is titrated through active production and destruction of related PTC-harbouring transcripts [32, 33]. Therefore, IIIa-TM transcripts could play important role/s in regulating the *normal* level of FGFR2 expression and signalling. However, when such transcripts persist, as in disease situations, they could assume entirely different regulatory roles.

It is not clear how and why IIIa-TM escapes NMD in FgfR2-IIIc$^{+/\Delta}$ tissues, but it is not a peculiarity of this allele as it can be detected in two other in vivo settings involving perturbed FGFR2 signalling. These are: (i) In FgfR2-IIIb null mice, which lack both copies of exon 8 (IIIb) and are deficient in *epithelial* FGFR2 signalling [34]; and, (ii) in some Pfeiffer syndrome patients who carry a mutation close to the splice acceptor site of FGFR2 exon 9 (IIIc) – the *mesenchymal* isoform - and manifest cranial and limb phenotypes [35]. The NMD pathway is not totally efficient [31] and it is possible that in the above scenarios, IIIa-TM is over-expressed above a threshold that NMD components, such as Upf1 enzyme, can deal with. Indeed, loss of Upf1 leads to persistence of PTC-containing transcripts [33]. However, the observed upregulation of IIIa-TM following perturbed FGFR2 signaling in multiple settings and tissue compartments, suggests that FGFR2 signalling itself somehow impacts the activity of NMD machinery to result in the stabilization of IIIa-TM, and possibly other PTC-containing transcripts.

Bioavailability of ligands is a key regulator of paracrine cell signalling levels and can be controlled through sequestration of ligands by soluble proteins. For example, the levels of EGF and Wnt signalling are controlled in part by naturally occurring extracellular proteins, Argos [36] and Frizzled-related proteins [37], respectively. Experimental over-expression of soluble FGFR2-IIIb in mice yields phenotypes that are reminiscent of loss of FgfR2-IIIb or Fgf10 genes themselves [1, 34, 38]. Indeed, soluble receptors are more potent than dominant-negative

membrane-anchored receptors in attenuating FGF signalling [38]. Therefore, IIIa-TM may attenuate FGFR signalling by sequestering FGF ligands away from membrane-anchored FGFRs and/or by forming non-functional hetero-trimers with FGFRs and FGF ligands. Furthermore, the latter may interfere with normal trafficking of FGFRs, as suggested by our immunolabelling studies in Fig. 5.

The inhibitory effects of IIIa-TM may depend on its glycosylation and interaction with FGF ligands. IIIa-TM carries 8 putative glycoyslation sites and our data suggests that these are glycosylated in multiple orders in vitro (Figs. 2C) and in vivo (Figs 1C, 2D). Delineating the exact type and pattern of glycosylation of these species may shed more light on its functions since glycosylation of distinct residues on FGFRs can differentially promote or reduce their association with FGF ligands [39, 40].

Our BIAcore data shows that through an association with FGF1, soluble IIIa-TM forms a hetero-trimeric complex with both IIIb and IIIc isoforms of FGFR2. We used FGF1, a pan-FGFR activating ligand in these assays, but it would be informative to determine whether IIIa-TM preferentially associates with distinct FGF ligands as seen in truncated soluble FGFR1 molecules [17]. Our present data indicates that IIIa-TM interacts with IIIc-activating ligands and possibly even interferes with other FGFR subtypes. Notably, IIIa-TM attenuates FGFR signalling in 293T cells in the presence of FGF2, in a system where FGFs -4 and -9 are the only other endogenously produced FGFs (LW and MKH, unpublished observations). Furthermore, IIIa-TM attenuates FGF signalling in developing chick somites, which is dependant on FGF8 to FGFR1 signalling [26].

Relevance to Apert syndrome and cancer

AS is caused by dominant-acting FGFR2 molecules that operate entirely in a ligand-dependant manner [6]. AS is hallmarked by the fusion of craniofacial sutures and by limb abnormalities accompanied by other sporadic visceral and neural defects [41]. Individuals harbouring the same mutation can present different levels of phenotypic severity. Although the ethnological origin of patients is likely to influence the severity of their defects, it is also conceivable that other modulatory molecules such as IIIa-TM could contribute to specific defects. Two specific examples include cleft palate [42] and blind colon [41], phenotypes that are reminiscent of complete loss of FGF10 or FGFR2-IIIb signalling in mice [1, 43].

How can IIIa-TM induce loss of FGFR2 function when AS type mutations are thought to act in a gain-of-function manner? Normally, epithelial and mesenchymal cells engage in a cross-talk through mutually-exclusive expression of FGFR2-IIIb and IIIc isoforms and their respective activating ligands (see Introduction; Supplementary Fig. 3). It has been shown that Apert mutant receptors act predominantly in the mesenchyme through an illegitimate interaction with FgfR2-IIIb-activating ligands, such as FGF10 [44]. Thus, membrane-anchored AS mutant receptors *and* up-regulated IIIa-TM combined, could compete with epithelially-expressed FgfR2-IIIb for its cognate ligand, FGF10, to cause a loss of FgfR2-IIIb function in epithelial cells. In support of this hypothesis, we have found that reducing the bioavailability of FGF10 in FgfR2-IIIc$^{+/\Delta}$ mice (i.e. in FgfR2-IIIc$^{+/\Delta}$; Fgf10$^{+/-}$ double mutants) accentuates this competition and results in the occurrence of blind colon and cleft palate in a significant number of double mutants (Supplementary Fig. 3; [23])

IIIa-TM may not be the only soluble receptor to becomes over-expressed in Apert patients [45]. Nonetheless, a detailed survey of these patients for IIIa-TM expression, together with experimental up-regulation of IIIa-TM in a spatially and

temporally-controlled manner in wild type and mutant mouse models would help delineate the roles we have postulated here.

Soluble FGFRs have been also been isolated from a variety of tumour cells [46-49]. Interestingly, a Pfeiffer syndrome type FGFR2 mutation that causes IIIa-TM up-regulation (described above)[35]), is also the cause of colorectal cancer [50]. It is not clear whether expression of soluble receptors such as IIIa-TM are the cause or the consequence of cancer, but our characterizations suggest IIIa-TM is likely to act as an inhibitor FGFR signaling in the context of tumorigenesis. It is interesting to note then that loss-of-FGFR2 function has been associated with specific types of astrocytomas and bladder cancers [51, 52].

ACKNOWLEDGEMENTS

We are very grateful to Drs. Charles Brearley and Saverio Brogna, and Prof. David Richardson for critical reading of the manuscript, and apologise to colleagues whose work could not be cited due to space limitations. This work was supported in part by a CRUK grant number: CA3094.

REFERENCES

1 Sekine, K., Ohuchi, H., Fujiwara, M., Yamasaki, M., Yoshizawa, T., Sato, T., Yagishita, N., Matsui, D., Koga, Y., Itoh, N. and Kato, S. (1999) Fgf10 is essential for limb and lung formation. Nat Genet. **21**, 138-141

2 Saito, T. and Fukumoto, S. (2009) Fibroblast Growth Factor 23 (FGF23) and Disorders of Phosphate Metabolism. International journal of pediatric endocrinology. **2009**, 496514

3 Meyers, E. N., Lewandoski, M. and Martin, G. R. (1998) An Fgf8 mutant allelic series generated by Cre- and Flp-mediated recombination. Nat Genet. **18**, 136-141

4 Naski, M. C., Wang, Q., Xu, J. and Ornitz, D. M. (1996) Graded activation of fibroblast growth factor receptor 3 by mutations causing achondroplasia and thanatophoric dysplasia. Nat Genet. **13**, 233-237

5 Hajihosseini, M. K. (2008) Fibroblast growth factor signalling in cranial suture development and pathogenesis. Frontiers of Oral Biology. **12**, 160-177

6 Wilkie, A. O. (2005) Bad bones, absent smell, selfish testes: the pleiotropic consequences of human FGF receptor mutations. Cytokine Growth Factor Rev. **16**, 187-203

7 McKeehan, W. L., Wang, F. and Kan, M. (1998) The heparan sulfate-fibroblast growth factor family: diversity of structure and function. Prog Nucleic Acid Res Mol Biol. **59**, 135-176

8 Beenken, A. and Mohammadi, M. (2009) The FGF family: biology, pathophysiology and therapy. Nature reviews. **8**, 235-253

9 Hajihosseini, M. K., Lalioti, M. D., Arthaud, S., Burgar, H. R., Brown, J. M., Twigg, S. R., Wilkie, A. O. and Heath, J. K. (2004) Skeletal development is regulated by fibroblast growth factor receptor 1 signalling dynamics. Development. **131**, 325-335

10 Tsang, M. and Dawid, I. B. (2004) Promotion and attenuation of FGF signalling through the Ras-MAPK pathway. Sci STKE. **2004**, pe17

11 Wheldon, L. M., Haines, B. P., Rajappa, R., Mason, I., Rigby, P. W. and Heath, J. K. Critical role of FLRT1 phosphorylation in the interdependent regulation of FLRT1 function and FGF receptor signalling. PloS one. **5**, e10264

12 Kuro-o, M. Klotho. Pflugers Arch. **459**, 333-343

13 Werner, S., Duan, D. S., de Vries, C., Peters, K. G., Johnson, D. E. and Williams, L. T. (1992) Differential splicing in the extracellular region of fibroblast growth factor receptor 1 generates receptor variants with different ligand-binding specificities. Mol Cell Biol. **12**, 82-88

14 Burgar, H. R., Burns, H. D., Elsden, J. L., Lalioti, M. D. and Heath, J. K. (2002)

Association of the signalling adaptor FRS2 with fibroblast growth factor receptor 1 (Fgfr1) is mediated by alternative splicing of the juxtamembrane domain. J Biol Chem. **277**, 4018-4023

15 Peters, K. G., Werner, S., Chen, G. and Williams, L. T. (1992) Two FGF receptor genes are differentially expressed in epithelial and mesenchymal tissues during limb formation and organogenesis in the mouse. Development. **114**, 233-243

16 Zhang, X., Ibrahimi, O. A., Olsen, S. K., Umemori, H., Mohammadi, M. and Ornitz, D. M. (2006) Receptor specificity of the fibroblast growth factor family. The complete mammalian FGF family. J Biol Chem. **281**, 15694-15700

17 Duan, D. S., Werner, S. and Williams, L. T. (1992) A naturally occurring secreted form of fibroblast growth factor (FGF) receptor 1 binds basic FGF in preference over acidic FGF. J Biol Chem. **267**, 16076-16080

18 Hanneken, A. (2001) Structural characterization of the circulating soluble FGF receptors reveals multiple isoforms generated by secretion and ectodomain shedding. FEBS Lett. **489**, 176-181

19 Maquat, L. E. (2005) Nonsense-mediated mRNA decay in mammals. J Cell Sci. **118**, 1773-1776

20 Hajihosseini, M. K., Wilson, S., De Moerlooze, L. and Dickson, C. (2001) A splicing switch and gain-of-function mutation in FgfR2-IIIc hemizygotes causes Apert/Pfeiffer-syndrome-like phenotypes. Proc Natl Acad Sci U S A. **98**, 3855-3860

21 Oldridge, M., Zackai, E. H., McDonald-McGinn, D. M., Iseki, S., Morriss-Kay, G. M., Twigg, S. R., Johnson, D., Wall, S. A., Jiang, W., Theda, C., Jabs, E. W. and Wilkie, A. O. (1999) De novo alu-element insertions in FGFR2 identify a distinct pathological basis for Apert syndrome. Am J Hum Genet. **64**, 446-461

22 Bochukova, E. G., Roscioli, T., Hedges, D. J., Taylor, I. B., Johnson, D., David, D. J., Deininger, P. L. and Wilkie, A. O. (2009) Rare mutations of FGFR2 causing apert syndrome: identification of the first partial gene deletion, and an Alu element insertion from a new subfamily. Hum Mutat. **30**, 204-211

23 Hajihosseini, M. K., Duarte, R., Pegrum, J., Donjacour, A., Lana-Elola, E., Rice, D. P., Sharpe, J. and Dickson, C. (2009) Evidence that Fgf10 contributes to the skeletal and visceral defects of an Apert syndrome mouse model. Dev Dyn. **238**, 376-385

24 Hajihosseini, M. K. and Dickson, C. (1999) A subset of fibroblast growth factors (Fgfs) promote survival, but Fgf-8b specifically promotes astroglial differentiation of rat cortical precursor cells. Mol Cell Neurosci. **14**, 468-485

25 Anderson, J., Burns, H. D., Enriquez-Harris, P., Wilkie, A. O. and Heath, J. K. (1998) Apert syndrome mutations in fibroblast growth factor receptor 2 exhibit increased affinity for FGF ligand. Hum Mol Genet. **7**, 1475-1483

26 Smith, T. G., Sweetman, D., Patterson, M., Keyse, S. M. and Munsterberg, A.

(2005) Feedback interactions between MKP3 and ERK MAP kinase control scleraxis expression and the specification of rib progenitors in the developing chick somite. Development. **132**, 1305-1314

27 Terada, M., Shimizu, A., Sato, N., Miyakaze, S. I., Katayama, H. and Kurokawa-Seo, M. (2001) Fibroblast growth factor receptor 3 lacking the Ig IIIb and transmembrane domains secreted from human squamous cell carcinoma DJM-1 binds to FGFs. Mol Cell Biol Res Commun. **4**, 365-373

28 Nelson, R. W., Nedelkov, D. and Tubbs, K. A. (2000) Biosensor chip mass spectrometry: a chip-based proteomics approach. Electrophoresis. **21**, 1155-1163

29 Miki, T., Bottaro, D. P., Fleming, T. P., Smith, C. L., Burgess, W. H., Chan, A. M. and Aaronson, S. A. (1992) Determination of ligand-binding specificity by alternative splicing: two distinct growth factor receptors encoded by a single gene. Proc Natl Acad Sci U S A. **89**, 246-250

30 Jones, R. B., Wang, F., Luo, Y., Yu, C., Jin, C., Suzuki, T., Kan, M. and McKeehan, W. L. (2001) The nonsense-mediated decay pathway and mutually exclusive expression of alternatively spliced FGFR2IIIb and -IIIc mRNAs. J Biol Chem. **276**, 4158-4167

31 Muhlemann, O., Eberle, A. B., Stalder, L. and Zamudio Orozco, R. (2008) Recognition and elimination of nonsense mRNA. Biochimica et biophysica acta. **1779**, 538-549

32 Lewis, B. P., Green, R. E. and Brenner, S. E. (2003) Evidence for the widespread coupling of alternative splicing and nonsense-mediated mRNA decay in humans. Proc Natl Acad Sci U S A. **100**, 189-192

33 Mendell, J. T., Sharifi, N. A., Meyers, J. L., Martinez-Murillo, F. and Dietz, H. C. (2004) Nonsense surveillance regulates expression of diverse classes of mammalian transcripts and mutes genomic noise. Nat Genet. **36**, 1073-1078

34 De Moerlooze, L., Spencer-Dene, B., Revest, J., Hajihosseini, M., Rosewell, I. and Dickson, C. (2000) An important role for the IIIb isoform of fibroblast growth factor receptor 2 (FGFR2) in mesenchymal-epithelial signalling during mouse organogenesis. Development. **127**, 483-492

35 Tsukuno, M., Suzuki, H. and Eto, Y. (1999) Pfeiffer syndrome caused by haploinsufficient mutation of FGFR2. J Craniofac Genet Dev Biol. **19**, 183-188

36 Klein, D. E., Nappi, V. M., Reeves, G. T., Shvartsman, S. Y. and Lemmon, M. A. (2004) Argos inhibits epidermal growth factor receptor signalling by ligand sequestration. Nature. **430**, 1040-1044

37 Kawano, Y. and Kypta, R. (2003) Secreted antagonists of the Wnt signalling pathway. J Cell Sci. **116**, 2627-2634

38 Celli, G., LaRochelle, W. J., Mackem, S., Sharp, R. and Merlino, G. (1998)

Soluble dominant-negative receptor uncovers essential roles for fibroblast growth factors in multi-organ induction and patterning. Embo J. **17**, 1642-1655

39 Duchesne, L., Tissot, B., Rudd, T. R., Dell, A. and Fernig, D. G. (2006) N-glycosylation of fibroblast growth factor receptor 1 regulates ligand and heparan sulfate co-receptor binding. J Biol Chem. **281**, 27178-27189

40 Polanska, U. M., Duchesne, L., Harries, J. C., Fernig, D. G. and Kinnunen, T. K. (2009) N-Glycosylation regulates fibroblast growth factor receptor/EGL-15 activity in Caenorhabditis elegans in vivo. J Biol Chem. **284**, 33030-33039

41 Cohen, M. M., Jr. and Kreiborg, S. (1993) An updated pediatric perspective on the Apert syndrome. Am J Dis Child. **147**, 989-993

42 Slaney, S. F., Oldridge, M., Hurst, J. A., Moriss-Kay, G. M., Hall, C. M., Poole, M. D. and Wilkie, A. O. (1996) Differential effects of FGFR2 mutations on syndactyly and cleft palate in Apert syndrome. Am J Hum Genet. **58**, 923-932

43 Fairbanks, T. J., De Langhe, S., Sala, F. G., Warburton, D., Anderson, K. D., Bellusci, S. and Burns, R. C. (2004) Fibroblast growth factor 10 (Fgf10) invalidation results in anorectal malformation in mice. J Pediatr Surg. **39**, 360-365; discussion 360-365

44 Ibrahimi, O. A., Zhang, F., Eliseenkova, A. V., Itoh, N., Linhardt, R. J. and Mohammadi, M. (2004) Biochemical analysis of pathogenic ligand-dependent FGFR2 mutations suggests distinct pathophysiological mechanisms for craniofacial and limb abnormalities. Hum Mol Genet. **13**, 2313-2324

45 Tanimoto, Y., Yokozeki, M., Hiura, K., Matsumoto, K., Nakanishi, H., Matsumoto, T., Marie, P. J. and Moriyama, K. (2004) A soluble form of fibroblast growth factor receptor 2 (FGFR2) with S252W mutation acts as an efficient inhibitor for the enhanced osteoblastic differentiation caused by FGFR2 activation in Apert syndrome. J Biol Chem. **279**, 45926-45934

46 Jang, J. H., Shin, K. H., Park, Y. J., Lee, R. J., McKeehan, W. L. and Park, J. G. (2000) Novel transcripts of fibroblast growth factor receptor 3 reveal aberrant splicing and activation of cryptic splice sequences in colorectal cancer. Cancer Res. **60**, 4049-4052

47 Takaishi, S., Sawada, M., Morita, Y., Seno, H., Fukuzawa, H. and Chiba, T. (2000) Identification of a novel alternative splicing of human FGF receptor 4: soluble-form splice variant expressed in human gastrointestinal epithelial cells. Biochem Biophys Res Commun. **267**, 658-662

48 Ezzat, S., Zheng, L., Yu, S. and Asa, S. L. (2001) A soluble dominant negative fibroblast growth factor receptor 4 isoform in human MCF-7 breast cancer cells. Biochem Biophys Res Commun. **287**, 60-65

49 Jang, J. H. (2002) Identification and characterization of soluble isoform of fibroblast growth factor receptor 3 in human SaOS-2 osteosarcoma cells. Biochem

Biophys Res Commun. **292**, 378-382

50 Jang, J. H., Shin, K. H. and Park, J. G. (2001) Mutations in fibroblast growth factor receptor 2 and fibroblast growth factor receptor 3 genes associated with human gastric and colorectal cancers. Cancer Res. **61**, 3541-3543

51 Ricol, D., Cappellen, D., El Marjou, A., Gil-Diez-de-Medina, S., Girault, J. M., Yoshida, T., Ferry, G., Tucker, G., Poupon, M. F., Chopin, D., Thiery, J. P. and Radvanyi, F. (1999) Tumour suppressive properties of fibroblast growth factor receptor 2-IIIb in human bladder cancer. Oncogene. **18**, 7234-7243

52 Yamaguchi, F., Saya, H., Bruner, J. M. and Morrison, R. S. (1994) Differential expression of two fibroblast growth factor-receptor genes is associated with malignant progression in human astrocytomas. Proc Natl Acad Sci U S A. **91**, 484-488

Table I: Summary of kinetic data for FGF1 binding in the absence or presence of a 10-fold excess of soluble IIIa-TM. [a] K_{on} and K_{off} were derived as described in Materials and Methods.χ^2 was <10% of R_{max} in all cases. [b] The apparent affinity, K_D, is equal to K_{off}/K_{on}. [c] NDB - No Discernable Binding.

Soluble Analyte	**Parameter**	**Analyte bound to C1 sensor chip** Value by Receptor isotype		
		IIIa-TM-Fc	FGFR2-IIIb-Fc	FGFR-2IIIc-Fc
FGF1	K_{on} (/M/s)[a]	NDB[c]	3.93×10^{6}	2.41×10^{6}
	K_{off} (/s)[a]	NDB	2.02×10^{-3}	1.7×10^{-3}
	K_D (M)[b]	NDB	5.14×10^{-10}	7.05×10^{-10}
FGF1 +	K_{on} (/M/s)[a]	1.77×10^{5}	3.48×10^{5}	2.75×10^{5}
IIIaTM	K_{off} (/s)[a]	1.2×10^{-2}	1×10^{-3}	2×10^{-3}
	K_D (M)[b]	6.8×10^{-8}	2.87×10^{-9}	7.27×10^{-9}

FIGURE LEGENDS

Fig. 1. Structure and detection of IIIa-TM in FgfR2-IIIc$^{+/\Delta}$ (mutant) mice.

A. Schematic representation of FgfR2 locus and the aberrant splicing of exon 7(IIIa) into 10(TM) which yields a PTC-containing transcript and a truncated protein with eight potential glycosylation sites (black circles). In lower panel: checked box, secretory signal sequence; bold line, contribution of TM exon; Star, termination codon. B, C. Detection of IIIa-TM transcript and protein in the mutant but not wild type (WT) brain. B, use of Primers P1 and P2 (positioned indicated in panel A) in RT-PCR reactions generates two products from mutant RNA. Note, neural tissue express the IIIc isoform of FgfR2 [24]. C, The detergent-soluble fractions of mutant brain tissue resolved on 2D-gels and immunoprobed with anti-FgfR2 antibodies. Two major 55 kDa products (pIs 5.1 and 6.3), and a minor 120 kDa (pI 4.3) product are evident. No spots were detected in blots of wild type tissue.

Fig. 2. Generation and biochemical characterization of recombinant IIIa-TM protein.

A. The recombinant IIIa-TM protein is fused to IgG-Fc domain to aid in the purification process, and carries a 3C-protease sensitive site (arrow head) to allow cleavage of the IgG-Fc domain. B. Recombinant Fc-3C-IIIa-TM is optimally detected in the supernatant of 293T cells, 60 hours post-transfection. C. SDS-Page analysis of purified IIIa-TM protein reveals distinct oligomeric complexes of 55 to 200kDa under non-reducing conditions (NR). Under reducing conditions (R), a single ~50kDa product is detected, which is reduced further to ~35kDa after deglycosylation by PNGase-F treatment (R+P, lane 3,) D, 2D-gel analysis over pI range 4-7 reveals that 293T-expressed IIIa-TM can exist in multiple glycosylated forms in the range of 55 to 60 kDa.

Fig. 3. Binding kinetics of recombinant IIIa-TM to FGF1

Sensograms depict the surface plasmon resonance analysis of FGF1 binding to immobilized Fc-3C-tagged IIIa-TM, FGFR2-IIIb, and FGFR2-IIIC ectodomains, in the absence (D-F) or presence (G-I) of free IIIa-TM. A-C, shows negligible binding of IIIa-TM alone to these ectodomains. Coloured boxes indicate the concentrations of IIIa-TM and FGF1 applied in each setting. Higher response units (RU, vertical axis) noted in G-I, in the presence of excess IIIa-TM (62.5 nM) there is a net increase in interaction of FGF1 with the immobilized FGFR molecules. The corresponding kinetic data are summarized in Table I. J, Determination of Theoretical R_{eq} values for FGF1-FGFR2 binding using four different analyte concentrations (grey boxes, 6.25-50 nm) and a Langmuir (1:1) model of binding for curve fitting. Data are mean (± s.e.m) of duplicates on the same chip and represent results from 3 separate chips.

Fig. 4. Exogenous IIIa-TM modulates the dynamics of FgfR signalling in 293T cells.

A (Upper panel) RT-PCR analysis using isoform-specific primers [20] shows that IIIc isoforms of FGFRs -1 and -2 predominate in 293T cells. This is further confirmed for FGFR2 (lower panel) as RT-PCR amplified IIIa-IIIb-TM and IIIa-IIIc-TM products using common primers from FGFR2 IIIa and TM exons, are digested by EcoRV, but not AvaI enzymes [34]. B, Stimulation of 293T cells with the cognate ligand (FGF2) induces a time-dependent ERK activation in control cells (*lower panel*, lanes 1-3), which is attenuated by exogenous IIIa-TM (*lower panel*, lanes 4-6). Data is representative of 3 independent experiments. C, Analysis of immunoprecipitated FGFR2 shows a marked reduction in level of receptor tyrosine phosphorylation in the

presence of IIIa-TM, after both 5 min and 30 min of FGF2 stimulation.

Fig. 5. Exogenous IIIa-TM interferes with trafficking of FGFR2.

A, Experimental paradigm and time-course of analysis. B-G, Differential localization of FGFR2 in transfected Cos7 cells after their stimulation with exogenous FGF2 (20ng/ml) Heparin (10μg/ml) and IIIa-TM (5μg/ml). In untreated or cells stimulated with FGF2 or IIIa-TM alone, FGFR2 co-localizes with late endosomes, marked by Lamp2 expression (open arrows in B-D and E). Combined FGF2 and IIIa-TM treatment, however, appears to trap much of the transfected FGFR2 at the cell membrane and reduce its co-localization with endosomomal compartment (closed arrows in F and G). Results are representative of three separate experiments. Scale bars, 10 μm. H, Quantitation of FGFR2/Lamp2 co-localization co-efficient (see methods) shows a significant reduction in transfected cells treated with IIIa-TM when compared to its absence. Data are mean ± SEM, n≥ 15 from two independent experiments. *p<0.05, and ***p<0.0001.

Fig. 6. IIIa-TM attenuates FGFR signalling in vivo.

A, photomicrograph of a chick embryo highlighting the region that was electroporated at stage 17 of chick embryonic development. Comparison of panels B and C, shows a clear down-regulation *Mkp3* gene expression (purple stain) following electroporation of embryos with IIIa-TM (B), but not GFP-encoding control plasmids (C). The brown stain in (C) is in situ hybridization stain for GFP to show the comparable domain of GFP transduction.

Biochemical Journal Immediate Publication. Published on 28 Feb 2011 as manuscript BJ20100884

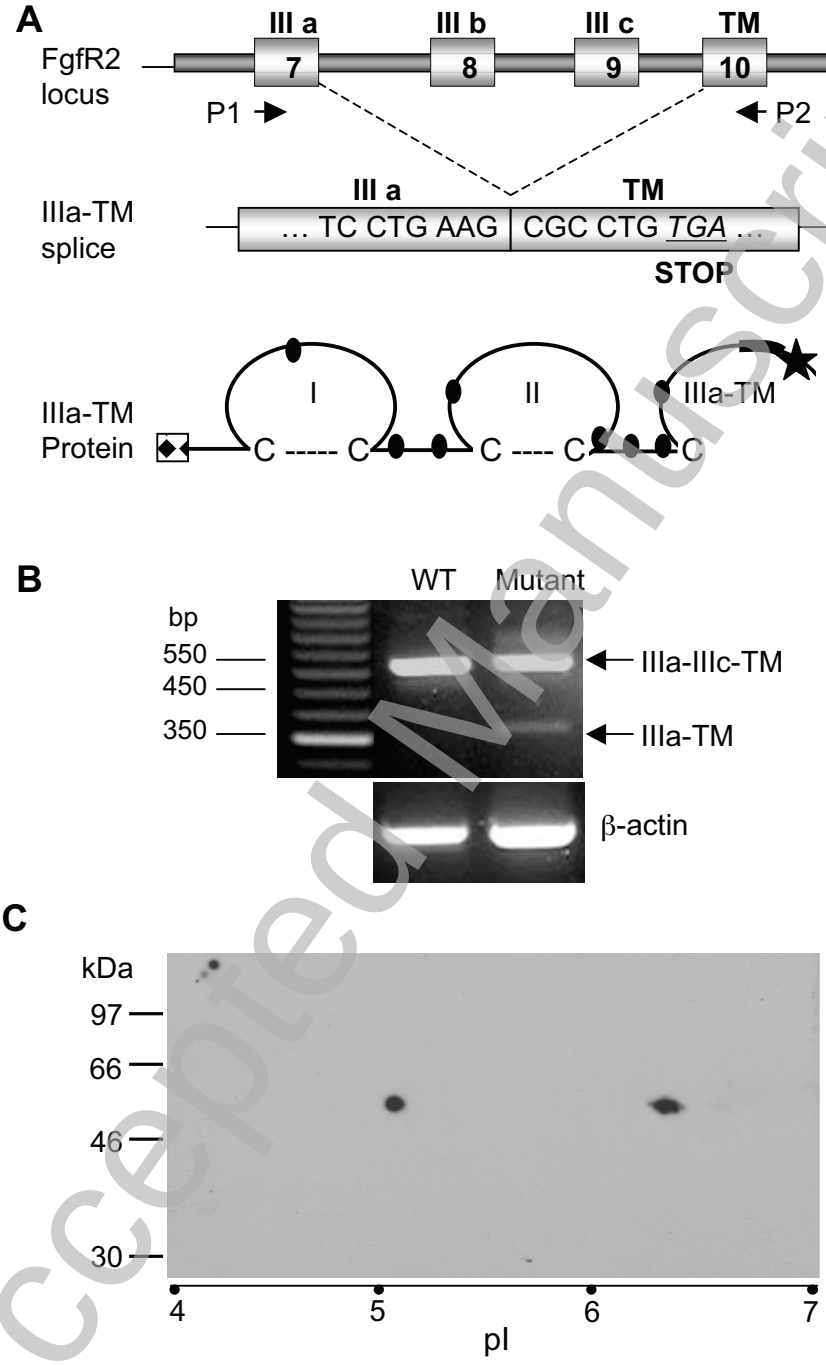

Biochemical Journal Immediate Publication. Published on 28 Feb 2011 as manuscript BJ20100884

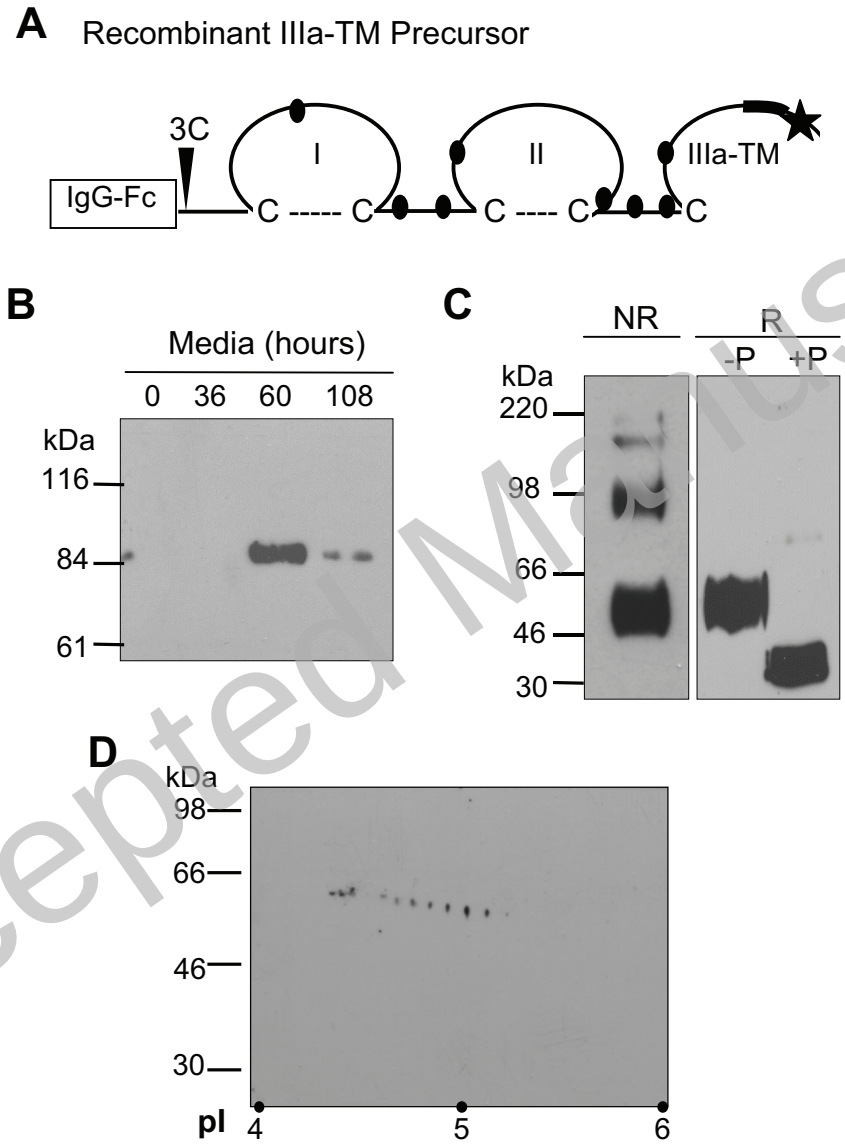

Biochemical Journal Immediate Publication. Published on 28 Feb 2011 as manuscript BJ20100884

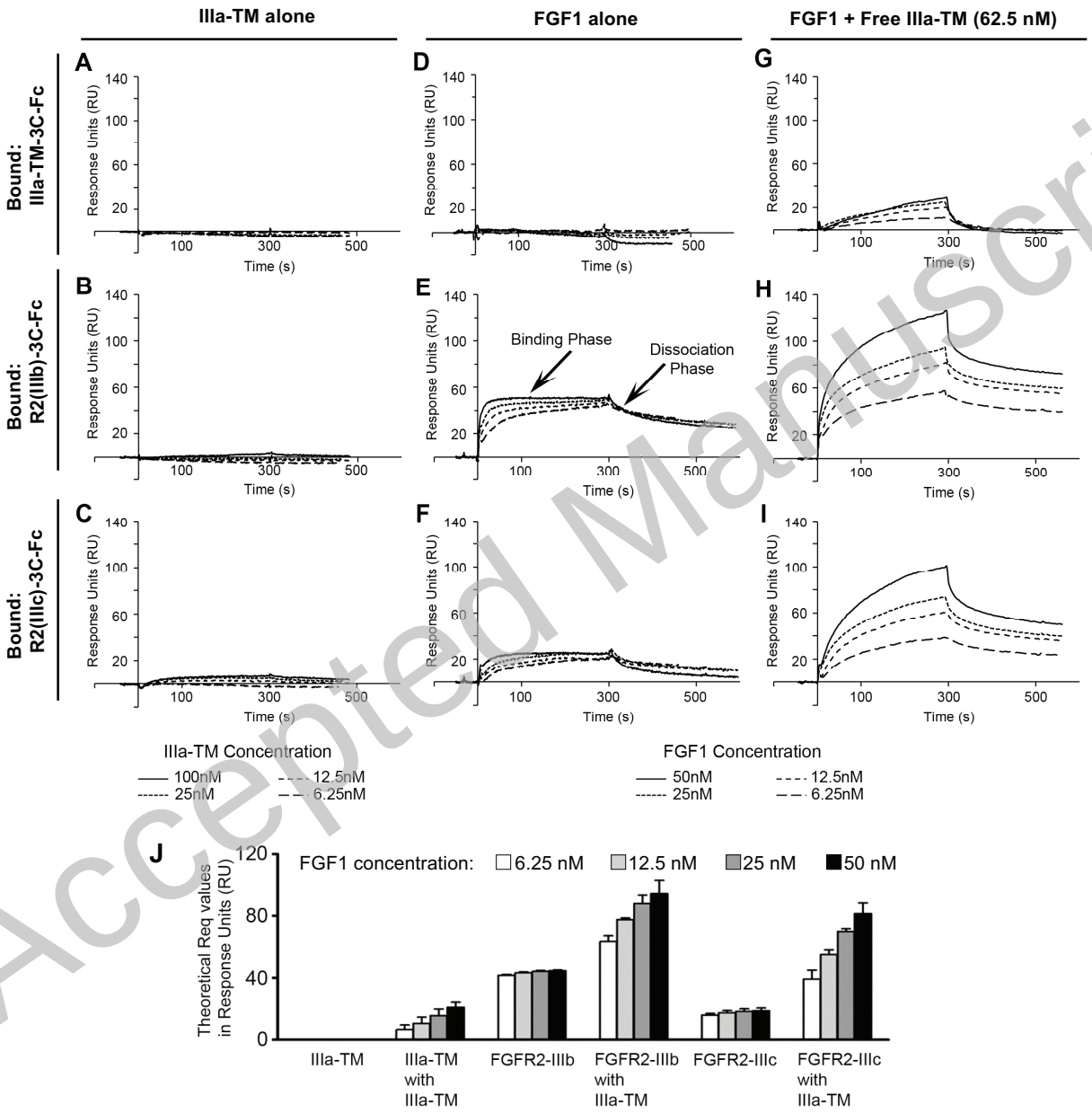

Biochemical Journal Immediate Publication. Published on 28 Feb 2011 as manuscript BJ20100884

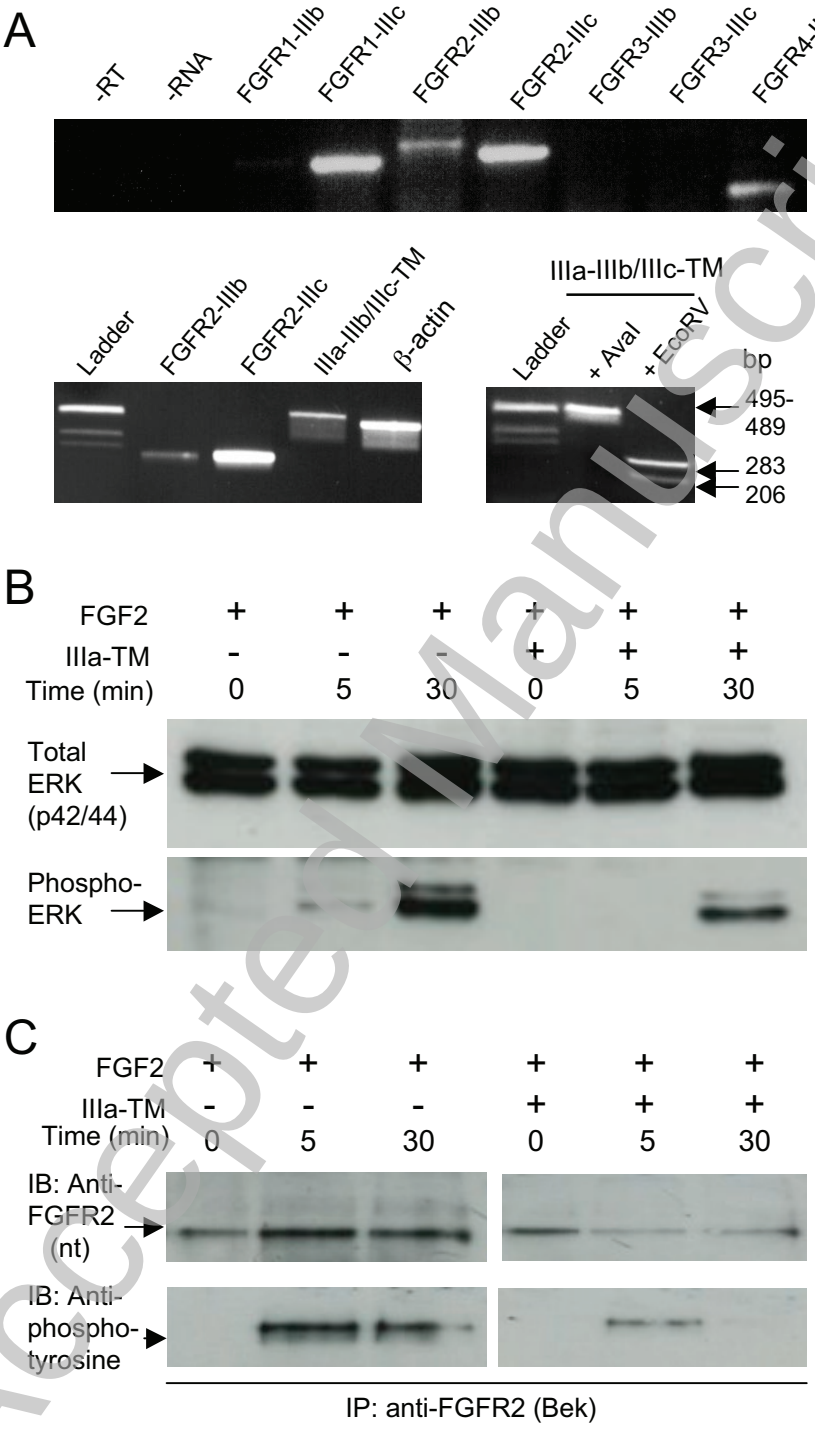

Biochemical Journal Immediate Publication. Published on 28 Feb 2011 as manuscript BJ20100884

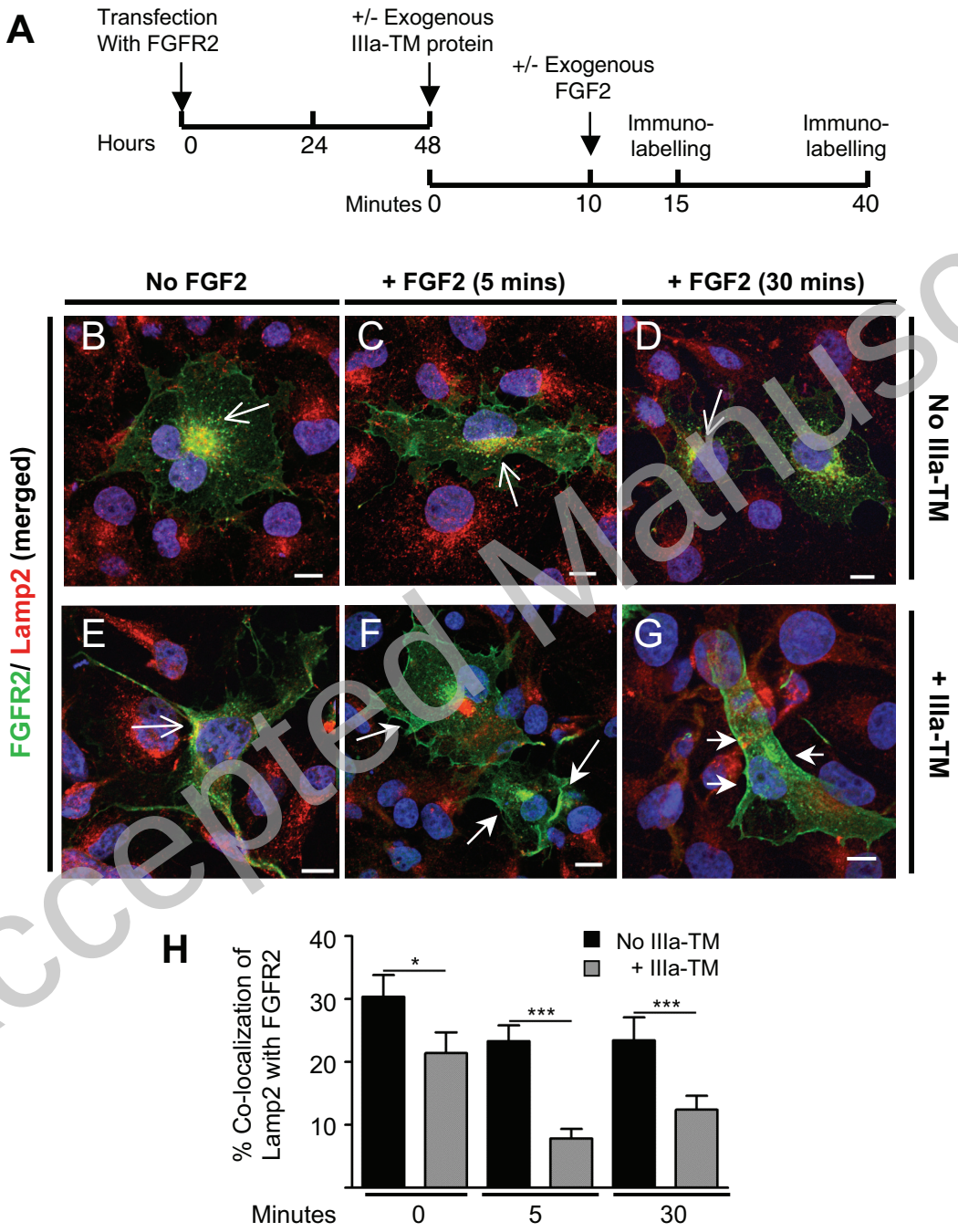

Biochemical Journal Immediate Publication. Published on 28 Feb 2011 as manuscript BJ20100884